International Journal of Greenhouse Gas Control, Volume 110, September 2021, Article number 103436
DOI:10.1016/j.ijggc.2021.103436

BLACK LIQUOR GASIFICATION WITH CALCIUM LOOPING FOR CARBON-NEGATIVE PULP AND PAPER INDUSTRY

by Mónica P. S. Santos, Vasilije Manovic, Dawid P. Hanak*

Abstract: Although considered one of the major energy-intensive industries (EIIs), the pulp and paper industry has also the potential for energy production from an industrial waste, black liquor. This study proposes black liquor gasification (BLG) coupled with calcium looping (CaL) as a CO_2 capture route for the pulp and paper industry. BLG with H_2 production (BLG-CaL-H2), BLG with gas turbine combined cycle (BLG-CaL-GT) or with solid oxide fuel cell (BLG-CaL-SOFC) were considered. The dependence of carbon capture and storage (CCS) cost on the natural gas, limestone, electricity imported and H_2 sale prices aside the expenditures related with BLG-CaL were evaluated. The CCS route, based on CaL retrofitted to the pulp and paper plant, was found to have a lower cost of CO_2 avoided (39.0 €/tCO_2) when compared with BLG-CaL (48.8–57.1 €/tCO_2). Between the BLG-CaL scenarios, BLG-CaL-H_2 presented the lowest cost of CO_2 avoided (48.8 €/tCO_2) but the highest energy penalty. Based on the thermodynamic performance, it was shown that CaL retrofit and BLG-CaL-SOFC presented the best overall performance, turning the electricity importer reference plant into electricity exporter. The economic sensitivity showed that the capital requirement of BLG-CaL has a strong effect on the cost of CO_2 avoided for all alternatives. The H_2 production is also strongly affected by the H_2 sale price while BLG-CaL-SOFC and BLG-CaL-GT are strongly dependent on natural gas price.

#gasification #carboncapture #technoeconomics #hydrogen

Dr Hanak Group
Solving global challenges via process engineering
For collaboration, contact us at contact@drhanak.com

Cite this paper: Santos, M.P.S., Manovic, V., and Hanak, D.P. (2021), Black liquor gasification with calcium looping for carbon-negative pulp and paper industry, International Journal of Greenhouse Gas Control, 110, 103436. DOI: 10.1016/j.ijggc.2021.103436

Published by Elsevier. This is the Author Accepted Manuscript issued with:
Creative Commons Attribution Non-Commercial No Derivatives License (CC:BY:NC:ND 4.0).
The final published version (version of record) is available online at DOI:10.1016/j.ijggc.2021.103436.
Please refer to any applicable publisher terms of use.

1. INTRODUCTION

To meet the ambitious targets set by the Paris Agreement, the net greenhouse gas (GHG) emissions must be zero or even negative between 2055 and 2080 (Fuss et al., 2014; Millar et al., 2017; Rogelj et al., 2018). As a result, the energy-intensive industries (EIIs) need to improve material and energy efficiencies, implement carbon capture and storage (CCS) technologies and reduce their dependence on fossil fuels (Gerres et al., 2019; McGrail et al., 2012). The development of clean energy sources and vectors, such as hydrogen, is of paramount importance (Spallina et al., 2019; Vogl et al., 2018). However, nearly all hydrogen is still produced from fossil fuel sources (International Energy Agency). Due to its abundance and carbon neutrality, biomass is considered to be an alternative feedstock in the energy sector (Sanna, 2014). The pulp and paper industry is one of the major consumers of biomass. Yet, this industry is still the fourth EII, contributing 4% of the total EU industry emissions in 2017 (Gerres et al., 2019). However, in contrast to other EIIs, the pulp and paper industry has the potential to become a carbon-negative industry on the integration of CCS (Santos et al., 2021).

Black liquor formed during the Kraft process is normally combusted in a recovery boiler to recover inorganic chemicals and produce process utilities (steam and electricity). Although the recovery boiler has been used for decades, this technology presents some drawbacks, such as low energy efficiency and health and safety issues such as smelt-water explosions and reduced-sulphur gas emissions (Larson et al., 2006; Whitty, 2005). Thus, technologies with improved efficiency and safety have been considered. Pressurised entrained flow gasification of black liquor, a technology developed by Chemrec AB, has been proven as a valid alternative to the recovery boiler. This technology has been demonstrated at the 3 MW_{th} LTU Green Fuels pilot plant in Piteå, Sweden (Jafri et al., 2016). As the alkali metals are present in black liquor, which have a catalytic effect, the produced syngas is characterised by low content of CH_4 and tars, even at short residence times and temperatures around 1000–1050 ℃ (Öhrman et al., 2012). As the smelt is dissolved in a quench bath at the bottom of the gasifier, the inorganic chemicals can be recovered as green liquor and recycled to the Kraft process. The techno-economic feasibility of black liquor gasification (BLG) for the production of biofuels (Andersson et al., 2014; Carvalho et al., 2018) and bulk chemicals, such as ammonia (Akbari et al., 2018), were reported. Andersson et al. (2014) assessed methanol production via black liquor gasification (BLG), Carvalho et al. (2018) studied methanol production via co-gasification with renewable feedstocks, such as pyrolysis liquid, crude glycerol and fermentation residues. The production of ammonia via BLG and co-gasification with pulp sludge or with waste sludge was evaluated by Akbari et al. (2018). However, the economic assessment of the integration of BLG with CO_2 capture (BLG-CCS) is still limited.

Zhang et al. (2011) have carried out a preliminary feasibility assessment of the integration of a BLG polygeneration system for the production of methanol, steam and electricity to a pulp and paper plant. This study also compared the BLG combined cycle with (BLG-CC-CCS) and without CO_2 capture (BLG-CC-NCC). The former considered both pre-combustion physical absorption (Selexol) from syngas and oxy-combustion of the unreacted gas from methanol

synthesis. Their study concluded that the BLG polygeneration system achieved a higher first law efficiency (34.1%) than the reference pulp and paper plant (15.7%). Moreover, BLG-CC--CCS based on oxy-combustion showed a lower net energy penalty (4.0%) and CO_2 capture cost (26.3 €/tCO_2) than that of the Selexol process (a net energy penalty of 6.5% and 40.9 €/tCO_2). Pettersson and Harvey (2012) have assessed the techno-economic performance of the BLG polygeneration system for the production of dimethylether (DME) and electricity. This study compared the implementation of different BLG concepts and evaluated the economic performance based on the net annual profit and potential of CO_2 emission reduction under different energy market scenarios. The BLG with DME production was shown to be the most attractive option among the considered scenarios. The BLG with electricity generation in pulp plant was still attractive under policies that promoted biofuels and high-penetration of low-carbon electricity. The integration of CO_2 capture with BLG in pulp plants and pulp and paper plants was also studied. It was shown to have a high potential for CO_2 emissions reduction, but the process profitability was strongly dependent on the CO_2 emission allowance price. Ferreira and Balestieri (2015) have compared the techno-economic performance of BLG-CC-CCS, which considered a conventional CO_2 absorption technology, and BLG-CC-NCC integrated to a pulp and paper plant. This study showed that the energy efficiency of the BLG-CC-NCC (34%) was higher than that for the BLG-CC-CCS (28%). The CO_2 avoided cost was shown to be around 20.5 €/tCO_2, which was estimated without considering the costs associated with CO_2 transport and storage. Moreover, Ferreira and Balestieri (2015) considered a carbon credit of 5.3 €/tCO_2 captured which implies that the economic feasibility of BLG-CC-CCS depends on incentives.

To date, the economic feasibility of the BLG coupled with CO_2 capture has been assessed for amine scrubbing, physical absorption and oxy-fuel combustion. However, the current literature presents limited information on the application of high-temperature solid looping cycles for BLG. Darmawan et al. (2018) considered chemical looping for the co-production of H_2 and electricity from BLG. Although their work proved that this approach is feasible from the thermodynamic standpoint, the economic feasibility of such a process needs to be assessed. Moreover, calcium looping (CaL) is an emerging high-temperature solid looping technology considered for thermochemical conversion of biomass. This technology can be either integrated with the thermochemical conversion process, so-called sorption-enhanced gasification (for solid biomass) or sorption-enhanced reforming (for gaseous or liquid biofuels) (Gil et al., 2015; Pfeifer et al., 2007; Wiranarongkorn and Arpornwichanop, 2017), in a single reactor, or can be integrated after the thermochemical conversion process in a secondary reactor (Armbrust et al., 2015; Connell et al., 2013; Müller et al., 2009). Although the pulp and paper process has an inherent CO_2 capture capability via CaL, as shown by Santos et al. (2021), no application of CaL for BLG has been considered.

For this reason, this work presents a comparative study between two different routes of CaL retrofit to the pulp and paper plant. The first route assumes that the existing Kraft process in the pulp and paper plant is retrofitted with CaL for CO_2 capture (Santos et al., 2021). The second route assumes that the BLG is integrated with CaL for simultaneous CO_2 capture and

Cite this work using DOI: 10.1016/j.ijggc.2021.103436

H_2 production (BLG-CaL) in the same reference plant. Three co-production routes are evaluated within BLG-CaL, considering BLG with H_2 production (BLG-CaL-H_2), BLG with gas turbine combined cycle (BLG-CaL-GT) or with solid oxide fuel cell (BLG-CaL-SOFC) for electricity production. The feasibility of the BLG-CaL routes is assessed considering the process thermodynamic and economic performance. Finally, a sensitivity analysis is carried out to evaluate the influence of costs on the economic performance.

Cite this work using DOI: 10.1016/j.ijggc.2021.103436

2. PROCESS MODELLING AND DESIGN

This study considered a retrofit of the reference pulp and paper plant with CO_2 capture and hydrogen. The process models were developed for the reference pulp and paper plant, CaL for CO_2 capture and BLG with CaL for simultaneous CO_2 capture and H_2 production. Overall, the techno-economic performance of the following cases was evaluated:

- Case 1 – reference pulp and paper plant
- Case 2 – calcium looping retrofit to the reference plant
- Case 3 – integrated black liquor gasification with calcium looping for H_2 production
- Case 4a – integrated black liquor gasification with calcium looping for power generation in gas turbine combined cycle
- Case 4b – integrated black liquor gasification with calcium looping for power generation in solid-oxide fuel cell

2.1. Reference pulp and paper plant

An integrated pulp and paper plant (Figure 1) considered by Santos et al. (2021)is considered as the reference case in this study. The energy and material balance essential to describe the reference plant was performed using CADSIM Plus®. The daily production capacity of this plant was assumed to be 1000 ADt (air-dried tonnes, containing 90% of dry solids), 375 ADt and 450 ADt of Kraft bleached pulp, thermochemical pulp and newsprint, respectively. Since the thermochemical pulp and part of bleached pulp are required in the newsprint process production, the market products include the total newsprint production and 925 ADt of Kraft bleached pulp. This translates into about 1810 t/d of black liquor solids (dry). Table 1 presents the black liquor composition. The fibre line, the calcium or lime cycle and the sodium or recovery cycle are the main components of the reference plant. The steam required to drive the process is produced in the recovery boiler and, partially, in the biomass and power boilers. The remaining steam is used for electricity generation in the steam turbine island. However, the electrical demand is higher than the amount of electricity generated in the steam turbine island. Therefore, an additional amount of electricity is imported from the electrical grid to meet the auxiliary requirements of the process.

Cite this work using DOI: 10.1016/j.ijggc.2021.103436

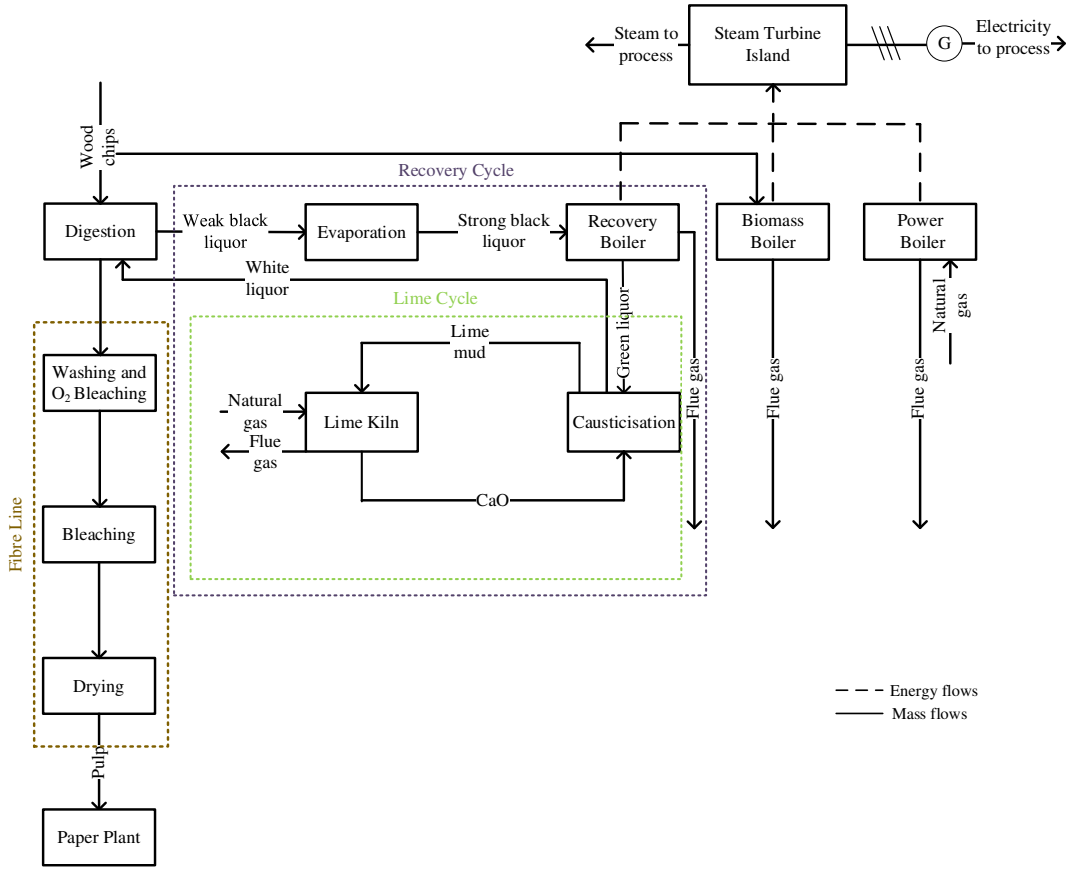

Figure 1. Simplified diagram of reference pulp and paper plant (Case 1).

Table 1. Black liquor composition

Properties	Value
Solids content [$\%_{wt}$]	74.0
Moisture content [$\%_{wt}$]	26.0
Elemental composition [$\%_{wt}$ db[1]]	C:36.1; H:3.5; O:34.2; Cl:0.4; Na:19.0; K:1.9; S:4.8
LHV[2] [MJ/kg, db]	12.37

[1]dry basis; [2]lower heating value

2.2. Calcium looping retrofit to the reference plant

As CO_2 emissions originate mostly from the biomass conversion, the reference plant can become carbon negative on CaL retrofit. Importantly, the lime mud from the Kraft process contains limestone and lime, the most commonly used sorbent in CaL. This implies an inherent CO_2 capture capability of the pulp and paper plants. Therefore, the CO_2 capture potential of the Kraft process was explored by retrofitting CaL in the lime cycle (Case 2). The approach to CaL retrofit in the existing Kraft process is shown in Figure 2. This concept has been described in detail by Santos et al. (2021) and the CaL model has previously been validated by Hanak et al. (2015). In such a concept, a larger kiln is used in place of the lime kiln in the reference plant. It is connected in parallel to the carbonator (RStoich reactor). It is assumed that such a

Cite this work using DOI: 10.1016/j.ijggc.2021.103436

modification does not influence the other stages of the Kraft process. The lime (CaO) produced from the calcination of the limestone ($CaCO_3$) in the lime kiln (Eq. (1)) is used to capture CO_2 produced in the recovery, power and biomass boilers in the carbonator (Eq. (2)). The heat required for sorbent regeneration is supplied via oxy-fuel combustion of natural gas in the calciner (RGibbs reactor). The properties and composition of flue gas streams are presented in Table 2.

$$\text{Calcination: } CaCO_3(s) \rightarrow CaO(s) + CO_2(g) \qquad \Delta H = 178 \text{ kJ/mol} \qquad (1)$$

$$\text{Carbonation: } CaO(s) + CO_2(g) \rightarrow CaCO_3(s) \qquad \Delta H = -178 \text{ kJ/mol} \qquad (2)$$

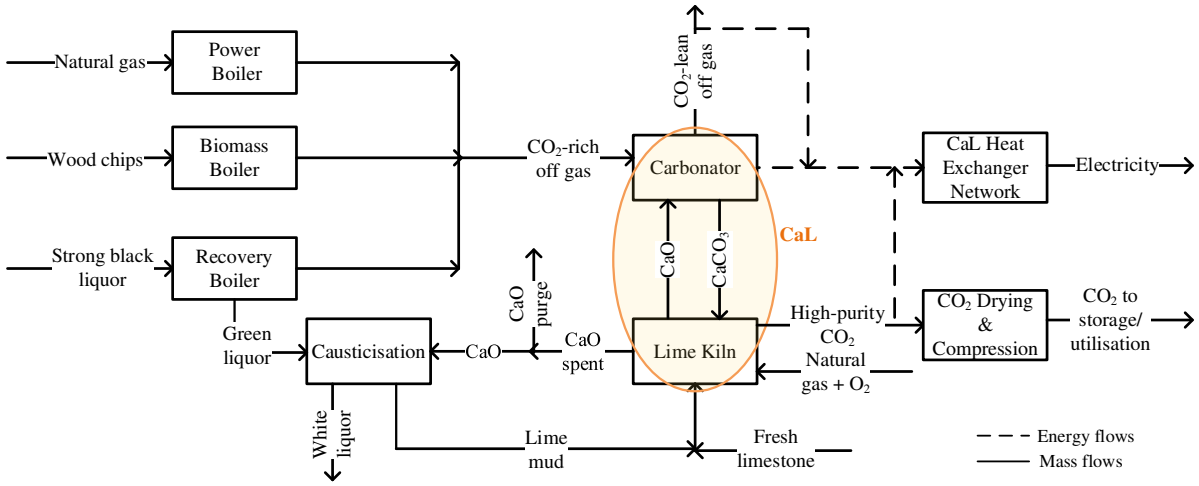

Figure 2. Simplified diagram of CaL retrofitted to the reference plant (Case 2).

2.3. Integration of black liquor gasification with calcium looping (BLG-CaL)

To explore the feasibility of BLG, the model for BLG integrated with CaL for H_2 production was developed and retrofitted with the reference plant. It should be noted that CO_2 produced from the power and biomass boilers (Table 2) is also captured in CaL. BLG was modelled using a Gibbs reactor in Aspen Plus®. To match the syngas composition under gasification conditions presented in Table 3, the BLG model was optimised and validated (Figure 3) with experimental data (Carlsson et al., 2010). It can be seen that the model predictions were in good agreement with the experimental data reported in the literature. The main design and operating conditions of the BLG-CaL process are presented in Table 3.

Cite this work using DOI: 10.1016/j.ijggc.2021.103436

Table 2. Summary of flue gas characteristic in reference pulp and paper plant (Santos et al., 2021)

Parameter	Power boiler	Recovery boiler	Hog boiler
Temperature [°C]	150.0	210.0	130.0
Mass flow rate [tonne/day]	330.3	11070.5	3957.0
N_2 [$\%_{vol}$]	71.7	63.5	56.6
O_2 [$\%_{vol}$]	0.7	1.7	0.8
H_2O [$\%_{vol}$]	18.4	21.4	29.8
CO_2 [$\%_{vol}$]	9.2	13.3	12.8
SO_x [ppm]	0.0	152.1	18.9

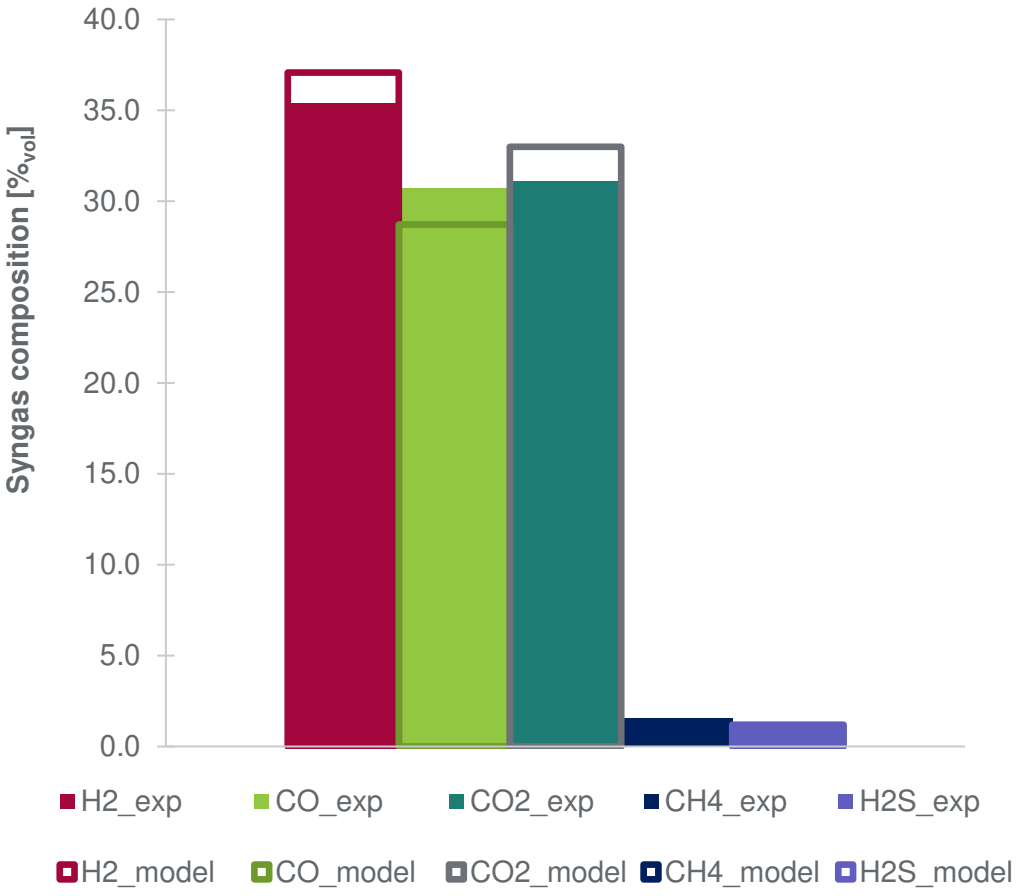

Figure 3. Black liquor gasification validation with literature data

Cite this work using DOI: 10.1016/j.ijggc.2021.103436

Table 3. Main modelling assumptions of the evaluated systems

Unit operation	Parameter	Value
Gasification	Temperature [℃]	1050
	Pressure [barg]	30
Calcium looping (Santos et al., 2021)		
Carbonator	Temperature [℃]	650.0
	Carbonated sorbent fraction [-]	0.7
	CO_2 capture efficiency in carbonator [%]	90.0
Lime kiln (Calciner)	Temperature [℃]	900.0
	Calcined sorbent fraction [-]	0.95
	Excess oxygen [$\%_{vol,dry}$]	2.5
	Relative make-up [-]	0.04
Gas cleaning	H_2S removal [%]	99.9
Pressure swing adsorption	H_2 recovery [%]	52.11
	H_2 purity [$\%_{vol}$]	99.99
	Tail gas pressure [bar]	1
	Delivery pressure [bar]	700 or 60
Steam Cycle (Santos et al., 2021)		
Live Steam	Temperature [℃]	593.0
	Pressure [bar]	154.0
High-pressure turbine	Isentropic efficiency [%]	92.0
	Mechanical efficiency [%]	99.8
Intermediate-pressure turbine	Isentropic efficiency [%]	77.5
	Mechanical efficiency [%]	96.5
Low-pressure turbine	Isentropic efficiency [%]	59.0
	Mechanical efficiency [%]	96.5
Second low-pressure turbine	Isentropic efficiency [%]	60.0
	Mechanical efficiency [%]	98.0
Condenser	Feed water temperature [℃]	10.0
CO_2 compression		
Compressors	Polytropic efficiency [%]	80.0
	Mechanical efficiency [%]	99.6
	Intercooler temperature [℃]	40.0
Pump	Isentropic efficiency [%]	80.0
	Mechanical efficiency [%]	99.6
CO_2 final stream	Temperature [℃]	25.0
	Pressure [bar]	110.0
	CO_2 purity [$\%_{vol}$]	≥ 95.0
Gas turbine	Compressor outlet pressure [bar]	20
	Combustor pressure drop [%]	2
	Turbine inlet temperature [℃]	1268
	Turbine isentropic efficiency [%]	80
	Turbine mechanical efficiency [%]	99.6
Solid oxide fuel cell	Temperature [℃]	910
	Pressure [bar]	1.08
	Fuel utilisation [%]	85
Reference conditions (Zhang et al., 2005)	Fuel composition [$\%_{vol}$] (H_2:67.0; CO:22.0; H_2O:11.0)	
	Fuel utilisation, U_f [%]	85
	Air utilisation, U_a [%]	25
	Temperature, T_{ref} [℃]	1000
	Pressure, P_{ref} [bar]	1
	Ratio of H_2 and H_2O partial pressures, $P_{H2,ref}/P_{H2O,ref}$	0.15
	O_2 partial pressure at cathode, $P_{O2,ref}$	0.164
Fresh material (Hanak et al., 2017)	Limestone composition [$\%_{wt}$] ($CaCO_3$:95.0; $MgCO_3$:3.5; SiO_2:0.6; Fe_2O_3:0.4; Al_2O_3:0.5)	
Fuel (Hanak et al., 2017)	Fuel [$\%_{vol}$] (CH_4:93.1; C_2H_6:3.2; C_3H_8:0.7, C_4H_{10}:0.4; CO_2:1.0; N_2 :1.6)	

Cite this work using DOI: 10.1016/j.ijggc.2021.103436

As this study aims to compare the techno-economic performance of two different CCS implementation routes in a pulp and paper plant, the three BLG alternatives were evaluated using a common design basis. The integration of CaL with BLG is represented in detail in Figure 4. This study considers the entrained flow gasifier (RGibbs reactor) that operates at elevated pressure and temperature, and uses oxygen as the gasifying agent. The concentrated black liquor is gasified at 30 barg and 1050 ℃. At such conditions, the main components of the syngas are H_2, CO_2 and CO (Figure 3). This temperature is controlled by the flowrate of the gasifying agent, for example, the oxygen obtained from the air separation unit (ASU). The gasifier is equipped with a quench section that enables the separation of the hot gas from the inorganic smelt (Jafri et al., 2016), which leaves the gasifier as green liquor and is returned to the Kraft process. The hot and pressurised gas is then expanded in a turbo-expander that is coupled with a generator to produce electricity. The CO_2 capture takes place in a secondary carbonator called water gas shift (WGS) carbonator (RGibbs reactor). This layout presents some benefits over sorption enhanced gasification (SEG). Since the system comprises the solids circulation between the interconnected carbonator and calciner, their operation at different pressures would not be desirable. Furthermore, if CaL is to operate at elevated pressure, the carbonator and the calciner will need to operate at higher temperatures. This will lead to enhanced sorbent degradation. Therefore, in the system comprising a separate gasifier and carbonator, the gasifier pressure and temperature can be increased as it is not restricted by the operating conditions of a carbonator (i.e. atmospheric pressure and 650 ℃). This is particularly important in BLG because at a low temperature (600 ℃), around 90% of the sulphur is gasified, producing H_2S in the gas phase. This affects the lime kiln balance since more Na is available as Na_2CO_3 (Larson et al., 2003). In this study, the WGS carbonator is integrated in parallel with another carbonator that captures the CO_2 from the flue gas produced in power and biomass boilers. As can be seen in Figure 4, the carbonation reaction, represented by Eq. (2), occurs in both carbonators. The CaO stream is split to achieve a CO_2 capture rate of 90% in both carbonators. Because CO_2 is captured in the WGS carbonator, the water gas shift reaction (WGSR), Eq. (3), is enhanced and a higher H_2 yield is achieved. Both $CaCO_3$ streams are then fed to a single calciner, where $CaCO_3$ is decomposed to CaO and a high-purity stream of CO_2 on heating, Eq. (1).

Water Gas Shift: $CO(g) + H_2O(g) \rightarrow CO_2(s) + H_2(g)$ $\Delta H = \pm 40.9$ kJ/mol (3)

Cite this work using DOI: 10.1016/j.ijggc.2021.103436

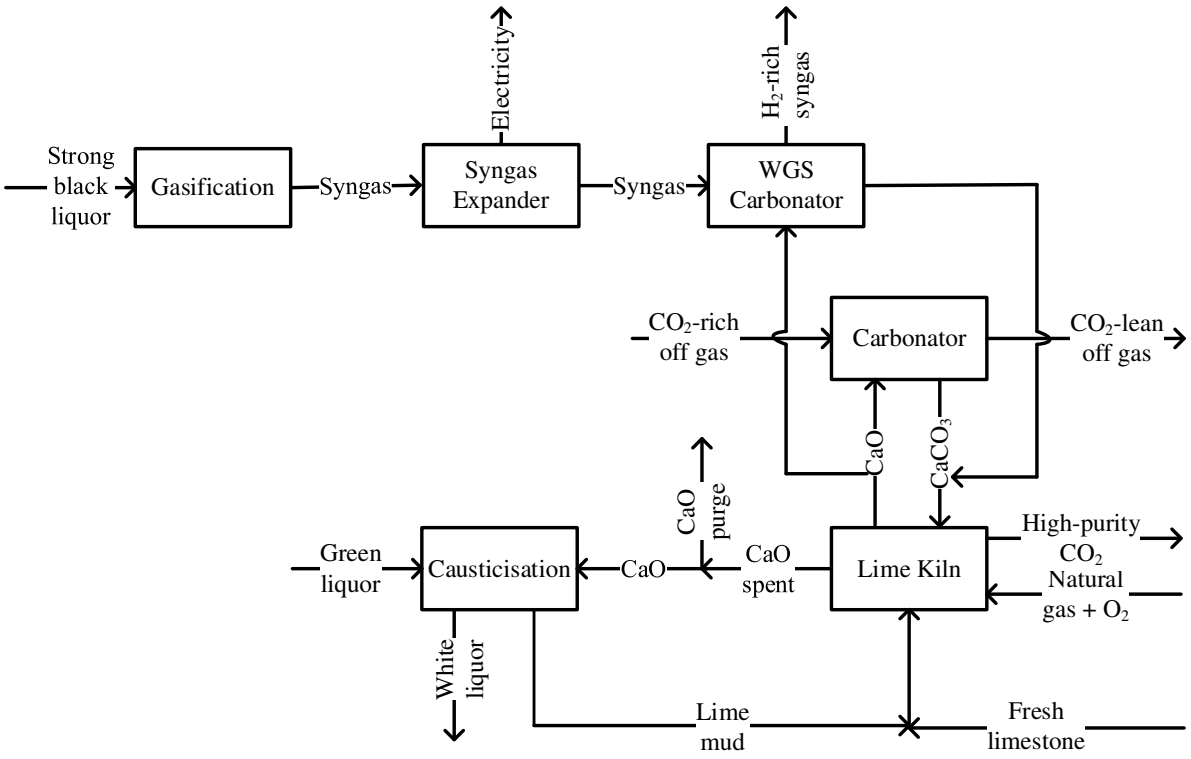

Figure 4. Detailed representation of calcium looping integration in the Kraft process for syngas upgrading

2.4. Retrofitted pulp and paper plant with calcium looping and BLG integrated with H_2 production

The H_2-rich syngas, along with the CO_2-lean off gas and high-purity CO_2 streams, are integrated in a heat exchanger network for steam production. The low-temperature H_2-rich syngas is then purified from H_2S (Sep separator), the sulphur is recovered in the Claus plant, and all the other minor contaminants in the pressure swing adsorption (PSA) unit (Sep separator). Although the PSA unit was not modelled in detail, it was assumed that it is a multi-column process that achieves 99.99% purity of H_2 with a recovery of 52.11% (Ribeiro et al., 2008). In this case (Case 3), two scenarios were considered, H_2 compression (MComp compressor) at 700 bar, transportation and storage (Case 3a) and H_2 available for immediate delivery at 60 bar (Case 3b). The latter assumes integration of the pulp and paper plant in an industrial hub with H_2 used as feedstock in the nearby industries. The conceptual design of this case is presented in Figure 5 and the operating conditions are reported in Table 3. It should be noted that the carbonators and calciner are represented by CaL block in Figure 5.

Cite this work using DOI: 10.1016/j.ijggc.2021.103436

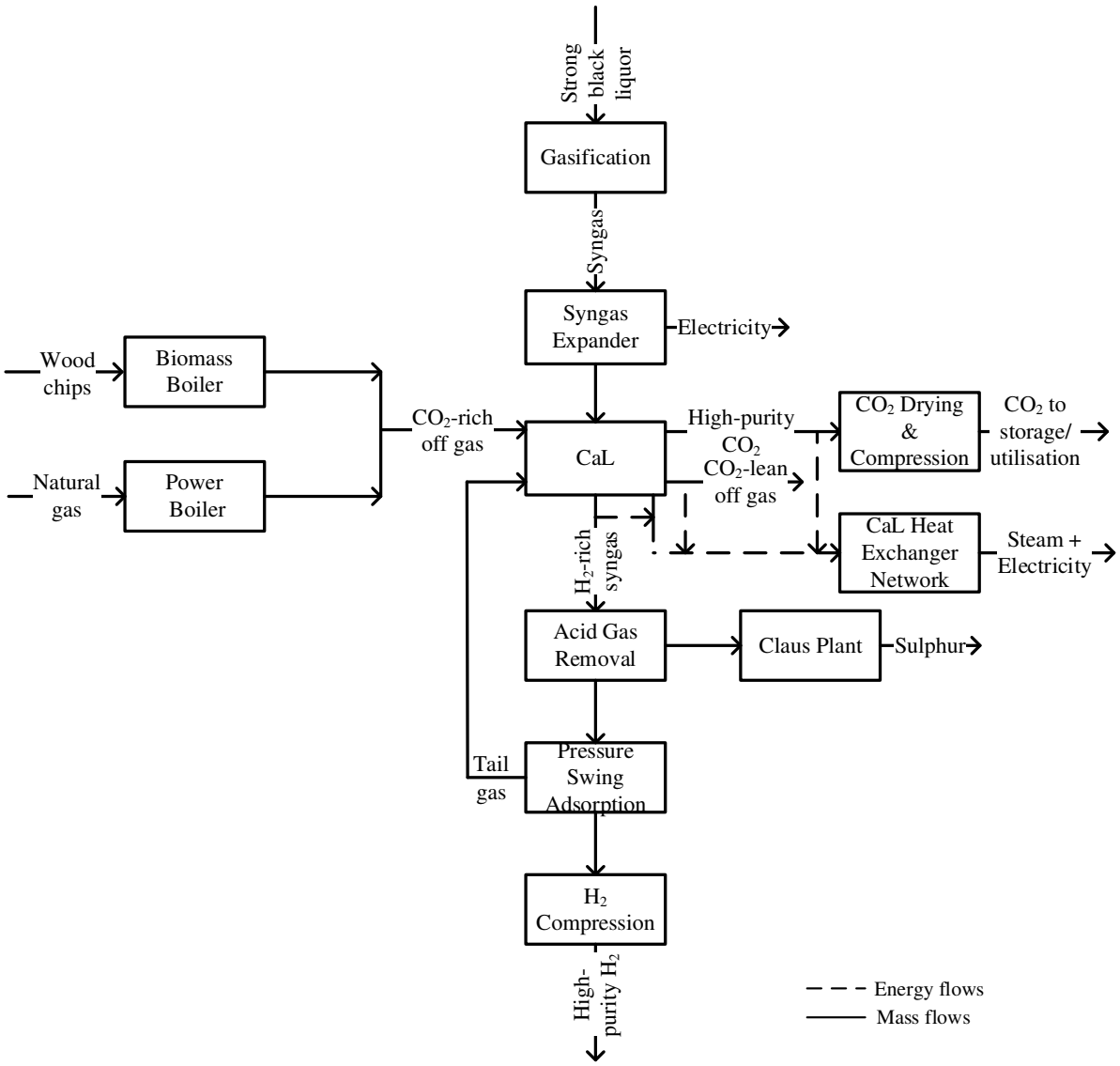

Figure 5. Simplified diagram of calcium looping and black liquor gasification integrated with H_2 production (Case 3).

2.5. Retrofitted pulp and paper plant with calcium looping and BLG integrated with GT combined cycle

In Case 4a, the H_2-rich syngas after H_2S removal is combusted in the gas turbine combustor (RGibbs reactor). As a result of H_2 combustion in the air, the resulting temperature of the flue gas is close to the adiabatic flame temperature (2229 ℃). It should be mentioned that the remainder of the steam produced in the heat exchanger network of CaL is expanded in a small steam turbine and fed to the combustor to increase the mass flow rate of the stream entering the expander. The exhaust gas is then mixed with bleed air from the air compressor (Comp compressor) to moderate the turbine inlet temperature to 1268 ℃. In the expander, the exhaust gas is expanded from 20 to 1 bar, generating electricity. This stream is then cooled in a heat

Cite this work using DOI: 10.1016/j.ijggc.2021.103436

exchanger, preheating the water for the steam turbine and thus, further contributing to generation of electricity. The schematic representation of this case and the operating conditions are given in Figure 6 and Table 3, respectively.

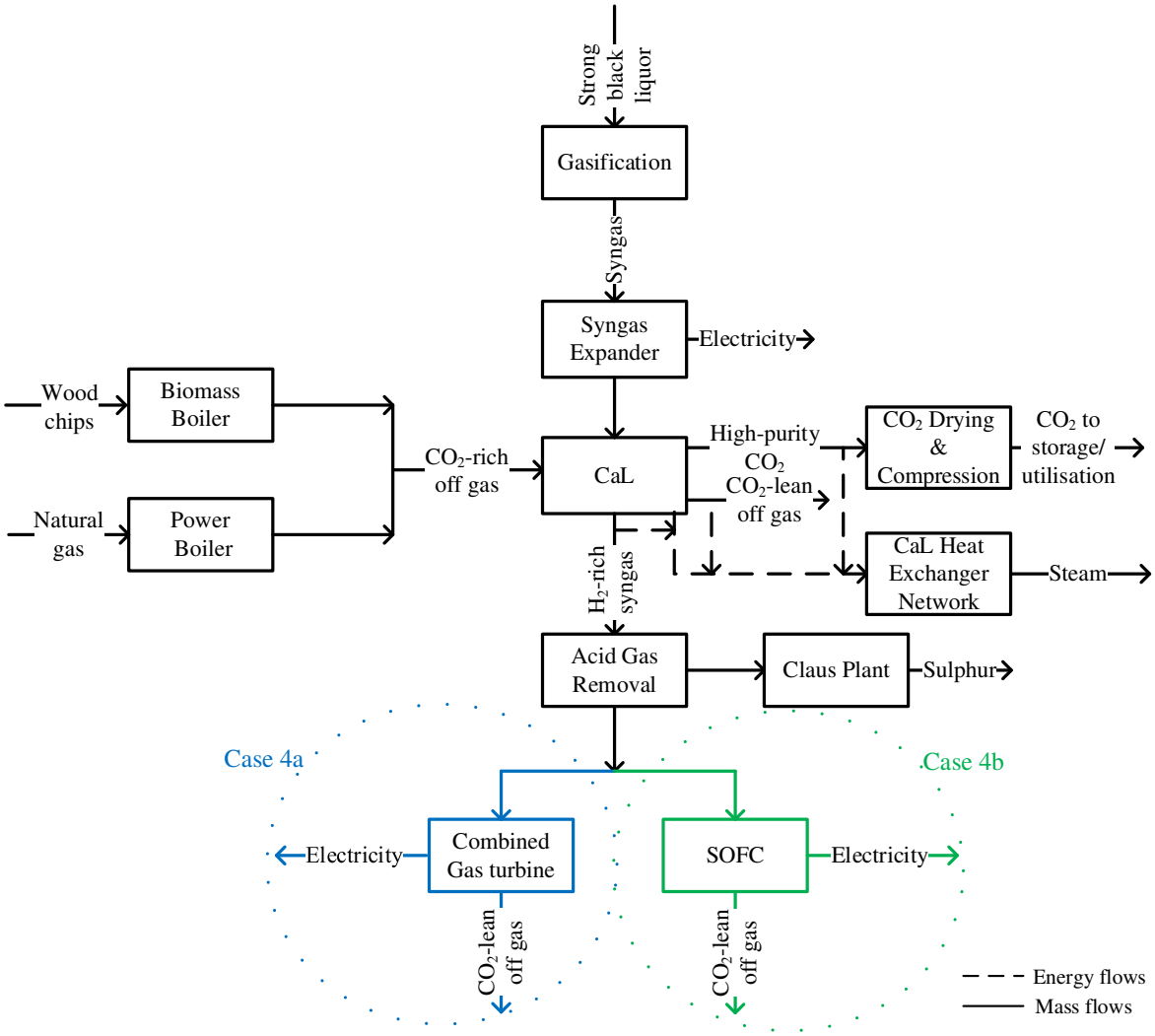

Figure 6. Simplified diagram of calcium looping and black liquor gasification integrated with GT combined cycle (Case 4a) or integrated with SOFC (Case 4b).

2.6. Retrofitted pulp and paper plant with calcium looping and BLG integrated with SOFC

Another case assessed in this work considers that the chemical energy of the H_2-rich syngas is converted to electricity in a solid-oxide fuel cell (SOFC) (Case 4b). Figure 6 presents a simplified diagram of this case. The operating conditions are summarised in Table 3. The heat available in the exhaust gas leaving the SOFC is then used to preheat water for steam production. This steam, along with the remaining steam generated in the CaL heat exchanger network, is expanded in the steam turbine for electricity generation. The SOFC process model was modelled in Aspen Plus® based on the model developed by Zhang et al. (2005) and Doherty et al. (2010). This model is described in detail and validated in Matuszny et al. (2020).

Cite this work using DOI: 10.1016/j.ijggc.2021.103436

3. TECHNO-ECONOMIC ANALYSIS

3.1. Parameters for thermodynamic assessment

The CCS and BLG cases presented above were compared with the reference case without carbon capture (Case 1), considering equivalent efficiency, gross power efficiency and net power efficiency as the key thermodynamic performance indicators.

The equivalent efficiency, Eq. (4), is defined as the ratio of the total useful energy outputs and the total energy inputs. The latter is defined as the total fuel consumed (natural gas, wood and black liquor) and, depending on the cases, the electricity imported. An electric efficiency of 45.9% is assumed to represent the electricity imported in terms of the fuel chemical energy input (De Lena et al., 2019). In this study, the equivalent efficiency uses the lower heating value to represent the energy content of fuels. The total useful energy outputs is represented as the sum of process steam produced in the system, net power output and, in Case 3, the chemical energy of high-purity H_2. In order to achieve a fair comparison, it is assumed that H_2 fuel cell with an electric efficiency of 47.9% (80% utilisation of H_2 and operating fuel cell voltage of 0.75 V) is used to convert H_2 into electricity (Mitsushima et al., 2018). Moreover, the energy available in the produced process steam was converted to electricity by assuming an electric efficiency of 45.9% (De Lena et al., 2019).

$$Equivalent\ efficiency = \frac{Total\ useful\ energy\ outputs}{Total\ energy\ inputs} \quad (4)$$

The gross power efficiency, Eq. (5), is defined as the ratio of the gross power output and the total energy inputs. The former is defined as the total power output of the integrated pulp and paper plant, considering the electricity produced in the expanders and steam cycle.

$$Gross\ power\ efficiency = \frac{Gross\ power\ output}{Total\ energy\ inputs} \quad (5)$$

The net power efficiency, Eq. (6), is defined as the ratio of the net power output and the total energy inputs. The difference between the gross power output and the net power output is that the latter accounts for the power requirement by the auxiliary equipment in the integrated pulp and paper plant.

$$Net\ power\ efficiency = \frac{Net\ electric\ power\ output}{Total\ energy\ inputs} \quad (6)$$

3.2. Parameters for economic assessment

Similarly to the thermodynamic assessment, three economic performance indicators were selected to assess the economic performance. This study uses the levelised cost of pulp (*LCOP*), the levelised cost of newsprint (*LCON*) and the cost of CO_2 avoided (*AC*) to quantify the economic performance of the considered cases (Santos et al., 2021). The levelised costs of products were estimated using the net present value method (*NPV*), presented in Eq. (7). The levelised costs correspond to the minimum prices for pulp and newsprint at which the NPV is zero. Under such condition, the project breaks even and the capital and operating costs

Cite this work using DOI: 10.1016/j.ijggc.2021.103436

associated with the specific case of the pulp and paper plant are equal to the revenues from the sales of the main products (pulp and newsprint) and by-products (electricity or hydrogen).

$$NPV = \sum_{t=1}^{n} \frac{CF_t}{(1+r)^t} - TCR \quad (7)$$

In Eq. (7), the discounted cash flow (CF_t) is estimated over the project lifetime (t), assuming a fixed project interest rate (r) and considering the total capital requirement (TCR). These parameters and other economic assumptions are presented in Table 4. Since inflation was not considered in this study, the material and feedstock prices, besides the market price of pulp and newsprint, were fixed during the project lifetime.

3.3. Cost estimation for the reference plant

The economic data reported by (Onarheim et al., 2017) was used to estimate the total capital investment and the operating costs of the reference plant. The capital cost was rescaled using the empirical correlation given by Eq. (8) where C represents the actual capital cost and S the scaling capacity factor. The reference value is denoted by the subscript 0. For capacity correction, a cost exponent (n) of 0.6 was assumed. The adopted economic methodology to estimate the capital and operating costs of the reference plant has been described in detail in Santos et al. (2021).

$$\frac{C}{C_0} = \left(\frac{S}{S_0}\right)^n \quad (8)$$

Cite this work using DOI: 10.1016/j.ijggc.2021.103436

Table 4. Economic model assumptions

Parameter	Value
BLG-CaL	
CaL fixed operating costs [€] (Martínez et al., 2014; Yang et al., 2010)	1.0% of TPC_{CaL}
CaL variable operating costs [€] (Martínez et al., 2014; Yang et al., 2010)	2.0% of TPC_{CaL}
BLG fixed and variable operating costs [€] (Andersson et al., 2016)	4.0% of TPC_{BLGU}
Gas cleaning fixed operating costs [€]	1.0% of TPC_{GC}[a]
Gas cleaning variable operating costs [€]	2.0% of TPC_{GC}[a]
Unit cost of electricity exported to the grid [€/MW_{el}h] (Onarheim et al., 2017)	40.0
Unit cost of electricity imported from the grid [€/MW_{el}h] (BEIS, 2019)	87.3
Natural gas unit cost [€/GJ] (Perry et al., 2007)	3.0
Limestone unit cost [€/t] (Lisbona et al., 2010; Martínez et al., 2014; Yang et al., 2010)	6.0
CO_2 transport and storage cost [€/t] (Romano et al., 2012)	7.0
Piping and integration costs indicator [%] (Michalski et al., 2019)	5.0
Others	
Expected lifetime [y] (Martínez et al., 2014; Yang et al., 2010)	25.0
Project interest rate [%] (Martínez et al., 2014; Yang et al., 2010)	8.8
Capacity factor [%] (Martínez et al., 2014; Yang et al., 2010)	80.0
Average USD/EUR exchange rate 2017 (Bank of England, 2019)	0.8898
Average GBP/EUR exchange rate 2017 (Bank of England, 2019)	1.1418
H_2 sale price [€/kg] (Eichman et al., 2016)	2.0

[a] In Case 3 this cost includes the costs associated with H_2 purification (PSA)

3.4. Cost estimation for CCS retrofit to reference plant

This work assesses the techno-economic performance of four CCS routes based on CaL and compares it with that of the reference case (Case 1). The economic evaluation carried out for Case 2 has been described in detail in Santos et al. (2021). Table 4 details the economic assumptions and prices used to account for the operating costs, whose for CaL do not include limestone and natural gas costs or the CO_2 transport and storage cost. Nevertheless, these were accounted for in the economic assessment. The Chemical Engineering Plant Cost Index (*CEPCI*) was used to estimate the price level of 2017 (CEPCI, 2020). If a different currency was used, an exchange rate of 0.8898 USD/EUR and 1.1418 GBP/EUR was assumed. The following economic assessment procedure applies to Case 3 and Case 4. In addition to the costs of CaL (C_{CaL}) and the BLG unit (C_{BLGU}), the total capital requirement of the capture plant, Eq. (9), also comprises the ASU cost (C_{ASU}), the CO_2 compression unit cost (C_{CCU}), the costs associated to the steam production (C_{SC}), the cost of gas cleaning (C_{GC}) and depending on the case, the cost associated with H_2 production and electricity generation by GT or SOFC (C_{Case_i}).

$$TCR_{cap} = C_{CaL} + C_{BLGU} + C_{ASU} + C_{CCU} + C_{GC} + C_{SC} + C_{Case_i} \quad (9)$$

As shown in Table 5, the O_2 flowrate and the brake power requirement were used to scale the C_{ASU} and C_{CCU}, respectively. The capital cost of CaL, BLGU, GC, SC and the costs associated with the GT, SOFC and H_2 production were estimated based on the sum of the costs of each component, given by Eq. (10) to Eq. (16). Except for C_{SC}, all the other costs account for the costs associated with piping and integration by assuming a cost indicator ($i_{P\&C}$) of 5% (Michalski et al., 2019). As the BLG conditions and the CO_2 capture rate is the same for the three cases (Case 3-4), the CaL, BLGU and GC capital costs are the same.

Cite this work using DOI: 10.1016/j.ijggc.2021.103436

$$C_{CaL} = (1 + i_{P\&C})(C_{calc} + C_{carb} + C_{FP} + C_{Fan} + C_{OXPH}) \quad (10)$$

$$C_{BLGU} = (1 + i_{P\&C})(C_{BLG} + C_{carb} + C_{SGE}) \quad (11)$$

$$C_{GC} = (1 + i_{P\&C})(C_{AGR} + C_{Claus}) \quad (12)$$

Besides the common capital costs, the H_2 production route also includes the costs associated with H_2 purification in PSA, C_{PSA}, and compression. To represent H_2 storage at 700 bar, the capital cost for compression to 700 bar, $C_{H_2 StorComp}$, and storage, $C_{H_2 PV}$ were considered. To represent H_2 transportation at 60 bar, the capital cost for compression to 60 bar, $C_{H_2 Comp}$, is accounted for, while the term $C_{H_2 PV}$ in Eq. (13) is eliminated.

$$C_{Case_3} = (1 + i_{P\&C})\left(C_{PSA} + C_{H_2 StorComp} + C_{H_2 PV}\right) \quad (13)$$

As shown in Eq. (14), the sum of a GT cost, C_{GT}, a steam turbine cost, C_{SST}, and a fuel compressor cost, C_{FC}, constitutes the capital cost associated with electricity generation in Case 4a.

$$C_{Case_{4a}} = (1 + i_{P\&C})(C_{GT} + C_{SST} + C_{FC}) \quad (14)$$

In Case 4b, the capital cost was estimated using Eq. (15) which, accounts for the individual cost of a SOFC stack, C_{SOFC}, and a DC/AC inverter, $C_{SOFC,DC/AC}$, an air compressor, C_{ArC}, and a fuel compressor, C_{FC}. In addition, 1% of the capital cost of the SOFC stack was also included for auxiliaries.

$$C_{Case_{4b}} = (1 + i_{P\&C})\left(C_{SOFC} + C_{SOFC,DC/AC} + C_{SOFC,aux} + C_{ArC} + C_{FC}\right) \quad (15)$$

The capital cost of the heat exchanger network, C_{SC}, is also estimated based on the individual cost of each component, as shown in Eq. (16). Because heat from the exhaust gas leaving the GT and SOFC is recovered to produce additional steam in the steam turbine island, the extra capital cost for two heat exchangers is accounted for. The correlations used to estimate these costs are summarised in Table 5.

$$C_{SC} = C_{HPW} + C_{ECON} + C_{LS} + C_{COND} + C_{HRSG} \quad (16)$$

The cost of CO_2 avoided (AC), represented by Eq. (17), depends on the levelised costs of pulp and newsprint, on the equivalent CO_2 emissions ($e_{CO_2,eq}$) of the reference and retrofitted plants and on the annual production rates, $\dot{m}_{Pulp}$ and $\dot{m}_{News}$.

$$AC = \frac{\left[\dot{m}_{Pulp}\frac{LCOP}{(\dot{m}_{Pulp}+\dot{m}_{News})} + \dot{m}_{News}\frac{LCON}{(\dot{m}_{Pulp}+\dot{m}_{News})}\right]_{cap} - \left[\dot{m}_{Pulp}\frac{LCOP}{(\dot{m}_{Pulp}+\dot{m}_{News})} + \dot{m}_{News}\frac{LCON}{(\dot{m}_{Pulp}+\dot{m}_{News})}\right]_{ref}}{e_{CO_2,eq,ref} - e_{CO_2,eq,cap}} \quad (17)$$

The equivalent CO_2 emissions ($e_{CO_2,eq}$), Eq. (18), accounts for the direct $\left(e_{CO_2}\right)$ and indirect $\left(P_e \cdot e_{CO_2,e}\right)$ CO_2 emissions. Since the indirect emissions are associated with the power generation of the imported electricity (P_e), they depend on the specific CO_2 emissions emitted by the power plant ($e_{CO_2,e}$). This figure was estimated based on the average power generation, excluding the combined heat and power (CHP), in the UK and the 27 EU Member States in 2015 (η_e=45.9% and $e_{CO2,e}$=262 $kg_{CO2}/MW_{el}h$) (De Lena et al., 2019). The direct and indirect

Cite this work using DOI: 10.1016/j.ijggc.2021.103436

CO_2 emissions considered in this study account only for the CO_2 released to the atmosphere as a result of the process operation and the CO_2 emissions associated with the energy carrier, respectively, following the approach by De Lena et al. (2019).

$$e_{CO_2,eq} = e_{CO_2} + Pe \cdot e_{CO_2,e} \quad (18)$$

If there is a surplus of electricity generated in the integrated pulp and paper plant, meaning that the retrofitted plant sells electricity to the electric grid, the indirect CO_2 emissions are deducted from the equivalent CO_2 emissions (De Lena et al., 2019).This has a favourable impact on the *AC.*

Cite this work using DOI: 10.1016/j.ijggc.2021.103436

Table 5. Summary of cost correlations used for capital cost estimation

Unit operation	Cost Correlation
Gasification unit [BL flowrate, , $\dot{m}_{BL}$ (t/d)] (Ekbom et al., 2003)	$C_{BLG} = 63.1e6\left(\frac{\dot{m}_{BL}}{3420}\right)^{0.7}$
Syngas expander [Brake power output, $\dot{W}_{SGE,BRK}$ (kW_{el})] (Manzolini et al., 2013)	$C_{SGE} = 33.7e6\left(\frac{\dot{W}_{SGE,BRK}}{200000}\right)^{0.67}$
Acid gas removal [Dry gas flowrate, $\dot{m}_{DG}$ (kg/s)] (Ekbom et al., 2003)	$C_{AGR} = 26.3e6\left(\frac{\dot{m}_{DG}}{37}\right)^{0.7}$
Claus sulphur plant [BL flowrate, $\dot{m}_{BL}$ (t/d)] (Ekbom et al., 2003)	$C_{Claus} = 6.6e6\left(\frac{\dot{m}_{BL}}{3420}\right)^{0.7}$
Air separation unit [O_2 production rate, $\dot{m}_{O2}$ (kg/s)] (Atsonios et al., 2013)	$C_{ASU} = 2.926e7\left(\frac{\dot{m}_{O2}}{28.9}\right)^{0.7}$
CO_2 compression unit [Brake power requirement, $\dot{W}_{CCU,BRK}$(kW_{el})] (Kreutz et al., 2005)	$C_{CCU} = 1.22914e7\left(\frac{\dot{W}_{CCU,BRK}}{13000}\right)^{0.67}$
Heat exchanger high-pressure water [Heat exchange area, A_{HPW} (m^2)] (Lee et al., 2014)]	$C_{HPW} = 130\left(\frac{A_{HPW}}{0.093}\right)$
Economiser [Heat exchange area, A_{ECON} (m^2)] (Lee et al., 2014)	$C_{ECON} = 130\left(\frac{A_{ECON}}{0.093}\right)$
Heat exchanger live steam [Heat exchange area, A_{LS} (m^2)] (Shirazi et al., 2012)	$C_{LS} = 2290(A_{LS})^{0.6}$
Heat exchanger condensate [Heat exchange area, A_{COND} (m^2)] (Lee et al., 2014)	$C_{COND} = 130\left(\frac{A_{COND}}{0.093}\right)$
Heat recovery steam generator [Heat exchange area, A_{HRSG} (m^2)] (Lee et al., 2014)	$C_{HRSG} = 130\left(\frac{A_{HRSG}}{0.093}\right)$
Oxygen preheater [Heat exchange area, A_{OXPH}(m^2)] (Lee et al., 2014)	$C_{OXPH} = 130\left(\frac{A_{OXPH}}{0.093}\right)$
Calciner [Calciner heat flux, $\dot{Q}_{calc}$ (kW_{th})] (Michalski et al., 2019)	$C_{calc} = 13140\,(\dot{Q}_{cal})^{0.67}$
Carbonator [Carbonator heat flux, $\dot{Q}_{carb}$ (kW_{th})] (Michalski et al., 2019)	$C_{carb} = 16591\,(\dot{Q}_{carb})^{0.67}$
Fuel preparation system [Fuel flowrate $\dot{m}_F$ (kg/s)] (Michalski et al., 2019)	$C_{FP} = 14158479\,(\dot{m}_F)^{0.24}$
Fan [Brake power requirement, $\dot{W}_{Fan,BRK}$ (kW_{el})] (Michalski et al., 2019)	$C_{Fan} = 103193\left(\frac{\dot{W}_{Fan,BRK}}{445}\right)^{0.67}$
Pressure swing adsorption unit [Inlet gas molar flowrate, $\dot{n}_{PSA}$ (kmol/h)] (Spallina et al., 2016)	$C_{PSA} = 27.96e6\left(\frac{\dot{n}_{PSA}}{17069}\right)^{0.6}$
H_2 compressor [Brake power requirement, $\dot{W}_{H_2,BRK}$ (kW_{el})] (Spallina et al., 2016)	$C_{H_2Comp} = 1200\left(\frac{\dot{W}_{H_2,BRK}}{0.746}\right)^{0.82}$
H_2 storage compressor [Brake power requirement, $\dot{W}_{H_2Stor,BRK}$ (kW_{el})] (Ni, 2006)	$C_{H_2StorComp} = 80\,\dot{W}_{H_2Stor,BRK}$
H_2 pressure vessel [H_2 mass, m_{H_2Stor} (kg)] (Ni, 2006)	$C_{H_2PV} = 40\,m_{H_2Stor}$
Gas turbine [Inlet air flowrate, $\dot{m}_{Air}$ (kg/s)] (DOE/NETL, 2014)	$C_{GT} = 31.5e6\left(\frac{\dot{m}_{Air}}{209}\right)^{0.85}$
Small steam turbine [Brake power output, $\dot{W}_{SST,BRK}$ (kW_{el})] (DOE/NETL, 2010)	$C_{SST} = 1.71e6\left(\frac{\dot{W}_{SST,BRK}}{1.65}\right)^{0.67}$
Solid-oxide fuel cell stack [Active area, A_{SOFC} (m^2); Operating temperature, T_{SOFC} (K)] (Shirazi et al., 2012)	$C_{SOFC} = A_{SOFC}(2.96T_{SOFC} - 1907)$
DC-to-AC inverter [Rated power output, $\dot{W}_{SOCF,DC}$ (kW_{el})] (Shirazi et al., 2012)	$C_{SOFC,DC/AC} = 1e5\left(\frac{\dot{W}_{SOCF,DC}}{500}\right)^{0.7}$
Solid-oxide fuel cell auxiliaries [Stack cost, C_{SOFC} (USD)] (Shirazi et al., 2012)	$C_{SOFC,aux} = 0.1\,C_{SOFC}$
Fuel compressor [Brake power requirement, $\dot{W}_{FC,BRK}$ (kW_{el})] (Lee et al., 2014; Shirazi et al., 2012)	$C_{FC} = 91562\left(\frac{\dot{W}_{FC,BRK}}{445}\right)^{0.67}$
Air compressor [Brake power requirement, $\dot{W}_{ArC,BRK}$ (kW_{el})] (Lee et al., 2014; Shirazi et al., 2012)	$C_{ArC} = 91562\left(\frac{\dot{W}_{ArC,BRK}}{445}\right)^{0.67}$

Cite this work using DOI: 10.1016/j.ijggc.2021.103436

4. RESULTS AND DISCUSSION

4.1. Thermodynamic assessment

The key outcomes from the thermodynamic analysis are presented in Figure 7. The steam demand of the reference plant, which remained constant for all the cases (132.6 kW_{th}/ADt), was met by a heat recovery steam generator (HRSG) that used the high-grade heat available in CaL. This shows the superior performance of CaL when compared with other CCS technologies, such as physical absorption that require an additional amount of steam to operate, resulting in a steam deficit if BLG is employed (Naqvi et al., 2013). The steam generated in CaL is combined with the steam produced by the power and hog boilers. It is then used to meet the steam requirement of the pulp and paper plant and produce electricity. As shown in the energy balance (Figure 7), Case 2 and Case 4b were the only cases with positive net power efficiency. As a result, the pulp and paper plant turned from an electricity importer to an electricity exporter, exporting 5.2 and 5.7 kW_{el}/ADt, respectively. It is important to note that although Case 4a had the highest gross power efficiency, the power requirement of the retrofitted pulp and paper plant was not fully met, resulting in an electricity deficit. To compensate for this deficit, 6.3 kW_{el}/ADt were imported from the electric grid. This can be explained by the high power consumption of the fuel gas and air compressors as these needed to be compressed to 20 bar to meet the operating requirements of the gas turbine. It was also found that the case with H_2 production, Case 3a and Case 3b, presented the lowest net power efficiency of around -7.0%. The negative value means that the electricity produced on-site did not meet the total power requirement, and thus, the pulp and paper plant needed to import electricity from the grid. This can be explained by the power requirement for H_2-enriched syngas purification and H_2 compression for delivery. Besides, electricity generation was penalised. Compression of H_2 at 60 bar, instead of at 700 bar and storage, reduced the specific electricity imported by 3.7%. The reference plant (Case 1) showed the best performance in terms of equivalent efficiency. This can be explained by an additional fuel consumption in CaL that increased the total energy input of the system.

Cite this work using DOI: 10.1016/j.ijggc.2021.103436

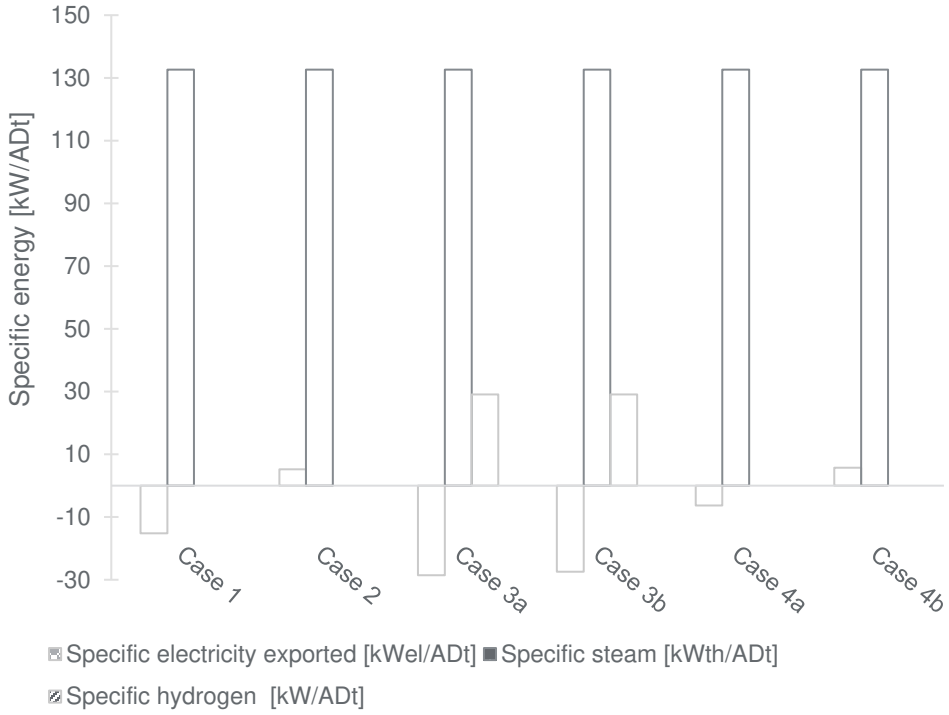

a)

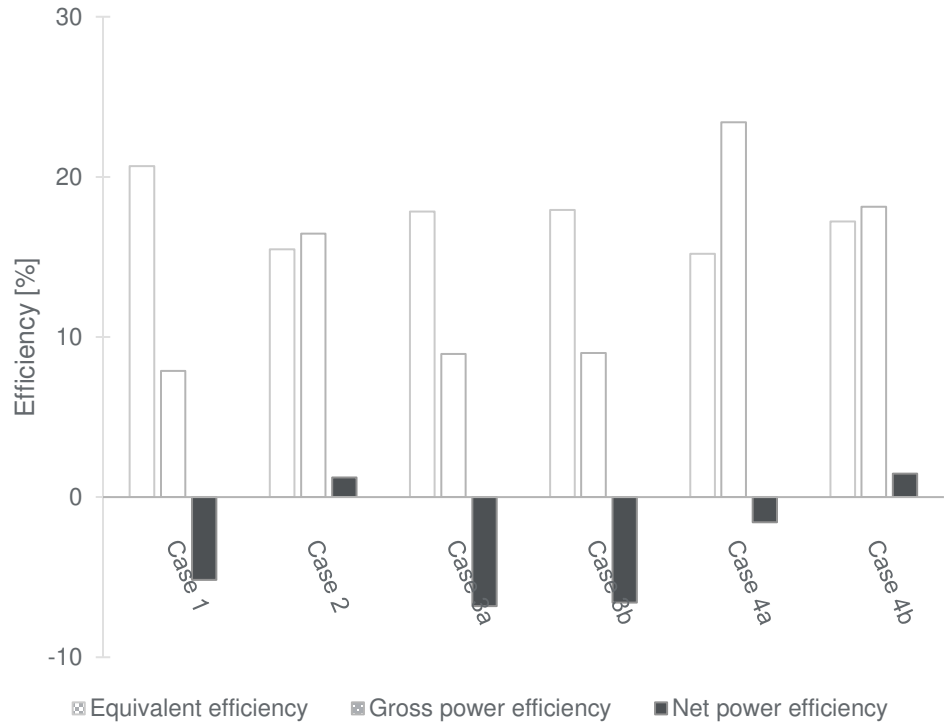

(b)

Figure 7. Comparative thermodynamic performance for (a) specific energy: electricity, steam and H_2 and (b) efficiency: equivalent, gross and net power.

Cite this work using DOI: 10.1016/j.ijggc.2021.103436

4.2. Economic assessment

The economic performance assessment (Figure 8) has revealed that Case 2 presented the lowest capital cost requirement, resulting in the lowest CO_2 avoided cost (39.0 €/tCO_2), followed by Case 3b (48.8 €/tCO_2). Although Case 3a and Case 3b showed the highest operation and maintenance (O&M) costs, which was around 0.6% higher in Case 3a (413 €/ADt) than in Case 3b (410.6 €/ADt), these costs were compensated by the additional revenue obtained from the H_2 sales. An H_2 sale price of 2 €/kg was assumed, which is a conservative assumption considering the H_2 sale price adopted by Eichman et al. (2016) , (2.7–8.9 €/kg). The O&M costs included the fixed and variable operating costs, the natural gas and limestone costs and, only in Case 3 and Case 4a, the costs associated with electricity import.

Considering the BLG-CaL cases, Case 3 and Case 4b showed lower costs of CO_2 avoided (50.8, 48.8 and 50.8 €/tCO_2, respectively) than that for Case 4a (57.1 €/tCO_2). This can be associated with the additional revenues obtained by the sales of H_2 (Case 3) and electricity (Case 4b). Importantly, the revenues from the pulp and newsprint sales are not represented in Figure 8 as these remained the same in all investigated cases. Though the cost of CO_2 avoided is higher in the BLG-CaL cases (Case 3 and Case 4) than that in the CaL retrofit case (Case 2, 39.0 €/tCO_2), it is still comparable to the results reported by Ferreira and Balestieri (2015) and Zhang et al. (2011). Zhang et al. (2011) presented the CO_2 capture costs on the CO_2 captured basis (26.3 and 40.9 €/tCO_2 for oxy-fuel combustion and Selexol, respectively) that are lower than the cost per CO_2 avoided. It should also be noted that figures reported in that study were estimated based on the capital costs reported in 2000 and 2005. The estimated CO_2 avoided cost (20.5 €/tCO_2) by Ferreira and Balestieri (2015) did not account for the cost of CO_2 transport and storage. It also considered a carbon credit for the CO_2 captured of 5.3 €/tCO_2. The costs in their work were also estimated based on capital costs reported in 2005, and therefore, the final cost of CO_2 captured will be underestimated compared to the results presented in this work. It also needs to be emphasised that in contrast to these studies, which only considered the CO_2 emissions from the BLG, this work considered CO_2 emitted by the entire pulp and paper plant.

Cite this work using DOI: 10.1016/j.ijggc.2021.103436

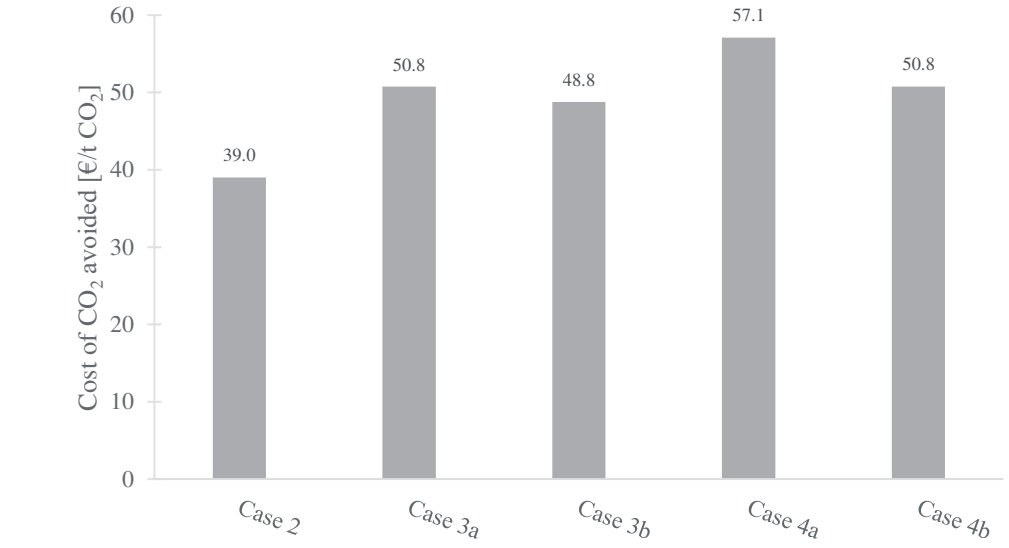

(a)

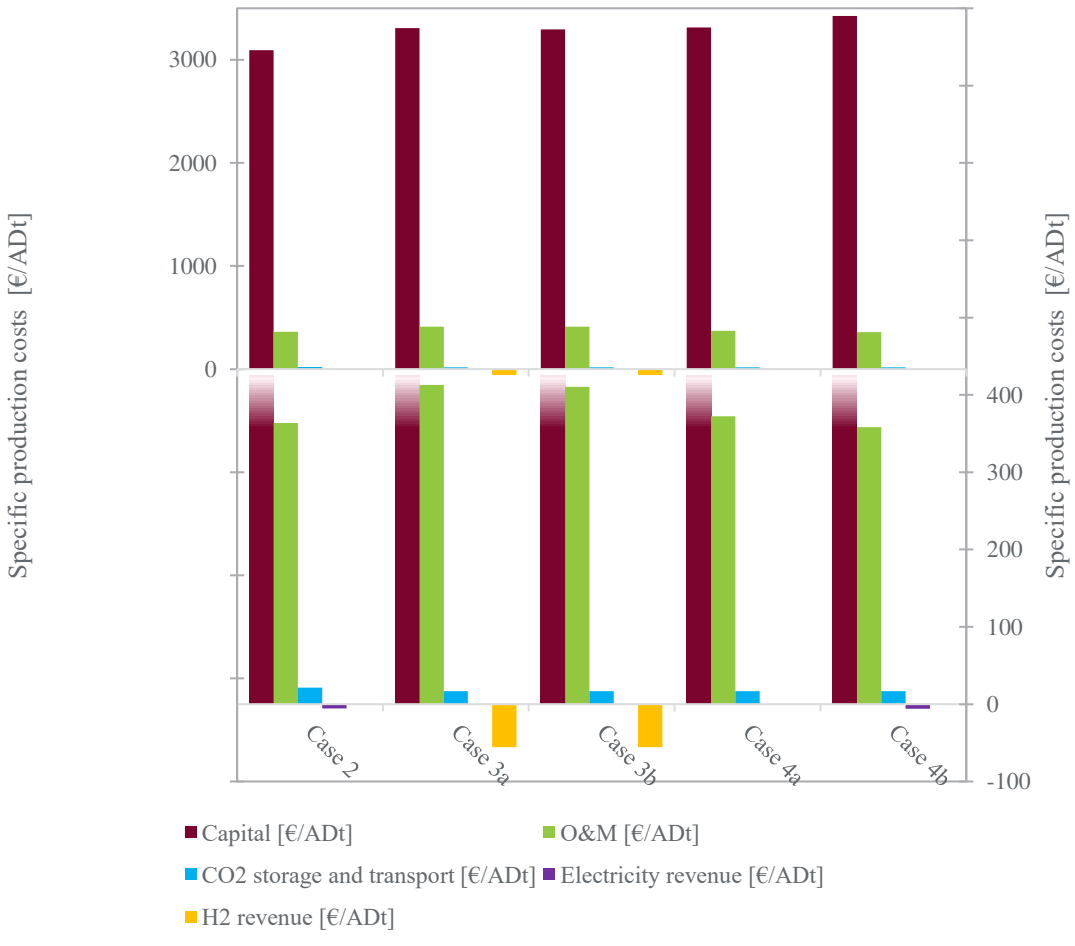

(b)

Figure 8. Economic case comparison of: (a) cost of CO_2 avoided and (b) specific production costs.

Cite this work using DOI: 10.1016/j.ijggc.2021.103436

4.3. Sensitivity analysis

To assess the dependence of CCS cost on various parameters and account for the uncertainty in the economic analysis, a sensitivity analysis was performed. The baseline figures for capital requirement, fixed and variable costs of BLG-CaL and the prices of H_2, natural gas, limestone, electricity imported, and CO_2 transport and storage were varied by ±25%. The subsequent change in the cost of CO_2 avoided is presented in Figure 9. It can be observed that the BLG-CaL capital requirement was the parameter that had a high impact in the investigated cases, changing from ±13.3% to ±17.2% in Case 4a and Case 4b, respectively. In Case 3, besides the BLG-CaL capital requirement, the CO_2 avoided cost is strongly dependent on the H_2 sale price, which in Case 3a had one percentage point higher impact on the CO_2 avoided cost than the BLG-CaL capital requirement. It was observed that a 25% increase of this parameter resulted in a reduction of around 15% in the cost of CO_2 avoided. On the other hand, a 25% reduction in the natural gas price, the second parameter with the highest influence on the CO_2 avoided cost in Case 4, caused a reduction in the cost of CO_2 avoided of 8.2% (Case 4a) and 8.9% (Case 4b), respectively. It should be noted that the reduction in the imported electricity price in Case 4b has a negative impact on the CO_2 avoided because only the reference plant imports electricity. Similarly to Case 2, the change in CO_2 avoided cost does not exceed 2% if the variable costs and limestone price rise 25%.

Cite this work using DOI: 10.1016/j.ijggc.2021.103436

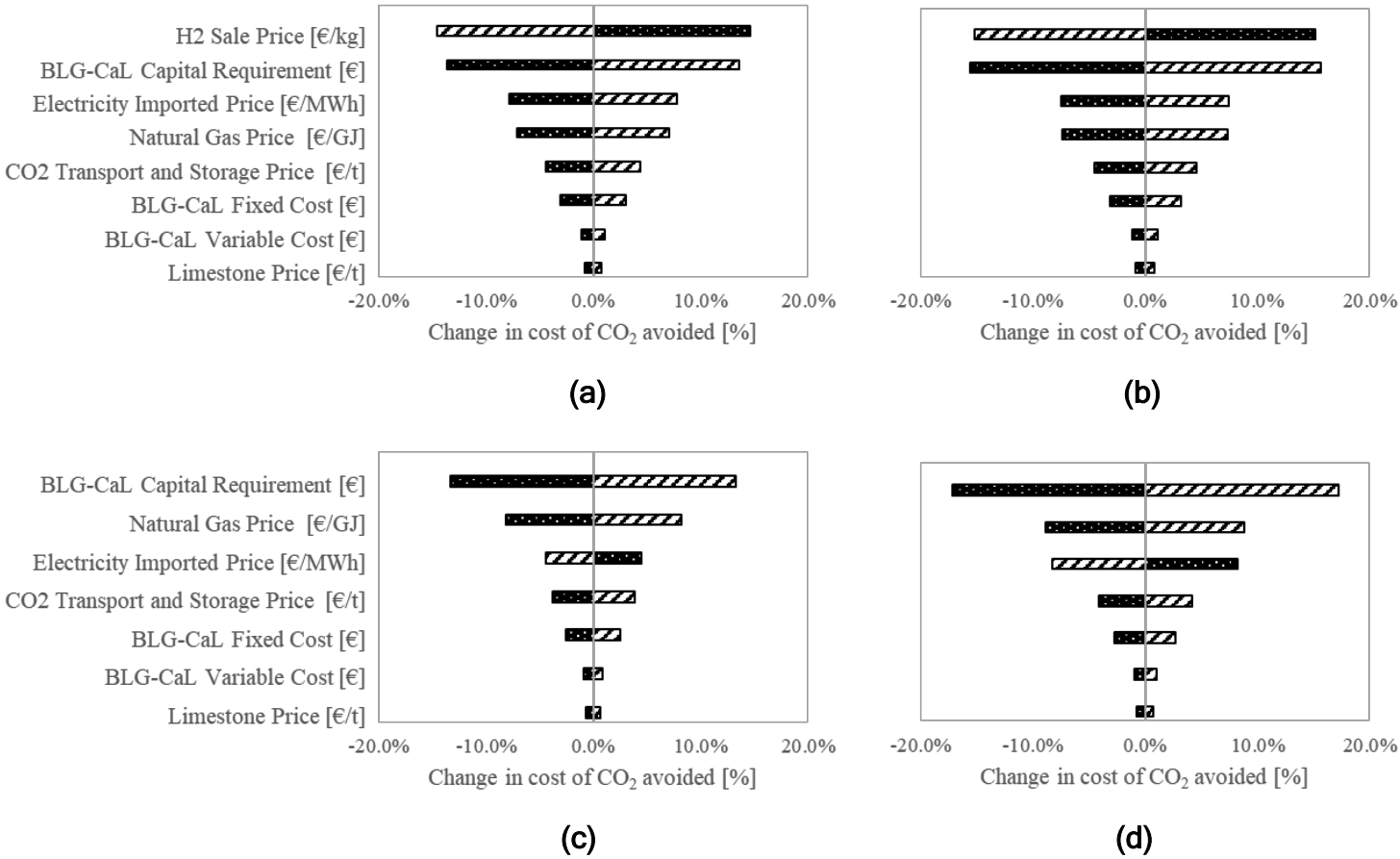

Figure 9. Effect of the main economic parameters on the cost of CO_2 avoided for (a) Case 3a, (b) Case 3b, (c) Case 4a and (d) Case 4b. Stripes: +25% of baseline parameter, Bubbles: -25% of baseline parameter

Cite this work using DOI: 10.1016/j.ijggc.2021.103436

5. CONCLUSIONS

This study aimed to compare two CCS routes, CaL and BLG-CaL, retrofitted to a pulp and paper plant. Three O_2-blown BLG coupled with CaL were assessed: BLG with H_2 (BLG-CaL-H_2) production, BLG with gas turbine combined cycle (BLG-CaL-GT) or with solid-oxide fuel cell (BLG-CaL-SOFC). The proposed configurations were assessed from the thermodynamic and economic points of view. It was shown that pulp and paper integrated with CaL and integrated with BLG with SOFC showed the best overall performance based on the thermodynamic indicators. In these two cases, the electricity importer reference plant turns into an electricity exporter. From an economic standpoint, the integration of CaL in the reference plant is characterised by the lowest cost of CO_2 avoided, 39.0 €/tCO_2. BLG-CaL was found to be a viable route for CCS; under the initial economic assumptions, BLG-CaL-H_2 presented the lowest cost of CO_2 avoided, 48.8 €/tCO_2, but the highest energy penalty since additional electricity import was required. On the other hand, BLG-CaL-SOFC presented the best net power efficiency, although it also had the highest capital cost requirement, with an estimated cost of CO_2 avoided of 50.8 €/tCO_2. Yet, the techno-economic results could be improved if the operating conditions of black liquor gasification are optimised. The impact of the uncertainty associated to the economic assumptions was also assessed, by varying the natural gas, limestone, electricity imported and H_2 sale prices as well as the costs associated to BLG-CaL. It was found that the capital requirement of BLG-CaL has a strong effect on the cost of CO_2 avoided for all alternatives. In Case 3, this is also strongly affected by the H_2 sale price while in Case 4, by the natural gas price.

ACKNOWLEDGEMENTS

This publication is based on research conducted within the “Clean heat, power and hydrogen from biomass and waste” project funded by UK Engineering and Physical Sciences Research Council (EPSRC reference: EP/R513027/1).

Cite this work using DOI: 10.1016/j.ijggc.2021.103436

NOMENCLATURE

A_j	area of heat exchange j [m^2]
AC	cost of CO_2 avoided [€/$t_{CO2avoided}$]
BLG	black liquor gasification
BLG-CaL	black liquor gasification with calcium looping
BLG-CaL-H_2	black liquor gasification with H_2 production
BLG-CaL-GT	black liquor gasification with gas turbine combined cycle
BLG-CaL-SOFC	black liquor gasification with solid oxide fuel cell
BLG-CC-CCS	black liquor gasification combined cycle with CO_2 capture
BLG-CC-NCC	black liquor gasification combined cycle without CO_2 capture
C_j	capital cost of equipment j [€]
CaL	calcium looping
$CEPCI$	Chemical Engineering Plant Cost Index
CCS	carbon capture and storage
CF_t	discounted cash flows through the project lifetime [€]
e	number of electrons produced per mole of H_2 [–]
e_{CO2}	direct CO_2 emissions from the pulp and paper plant [kg_{CO2}/ADt]
$e_{CO2,e}$	specific CO_2 emissions associated with power generation [$kg_{CO2}/MW_{el}h$]
$e_{CO2,eq}$	equivalent CO_2 emissions [kg_{CO2}/ADt]
GT	gas turbine
$i_{P\&C}$	piping and integration costs indicator [%]
$LCOP$	levelised cost of market product, pulp [€/ADt]
$LCON$	levelised cost of market product, newsprint [€/ADt]
LHV	lower heating value of the fuel [kJ/kg]
$\dot{m}_{Air}$	inlet air flowrate [kg/s]
$\dot{m}_{BL}$	black liquor flowrate [t/d]
$\dot{m}_{DG}$	dry gas flowrate [kg/s]
$\dot{m}_F$	fuel flowrate [kg/s]
m_{H_2Stor}	mass of H_2 for storage [kg]
$\dot{m}_{News}$	newsprint production per year [ADt/a]

Cite this work using DOI: 10.1016/j.ijggc.2021.103436

$\dot{m}_{O_2}$	O_2 production rate [kg/s]
$\dot{m}_{Pulp}$	pulp production per year [ADt/a]
n	cost capacity exponent [-]
$\dot{n}_{PSA}$	inlet gas molar flowrate [kmol/h]
NPV	net present value [€]
O&M	operation and maintenance
P_e	specific energy [$MW_{el}h$/ADt]
$P_{i,ref}$	reference partial pressure of component i in the gas mixture [bar]
P_{ref}	reference solid-oxide fuel cell operating pressure [bar]
PSA	pressure swing adsorption
$\dot{Q}_j$	heat flux of equipment j [kW_{th}]
r	discount rate [%]
S	scaling factor capacity [ADt/d]
SEG	sorption enhanced gasification
SOFC	solid-oxide fuel cell
t	project lifetime [y]
T_{ref}	reference solid-oxide fuel cell operating temperature [°C]
TCR	total capital requirement [€]
TIC	total installed cost [€]
TPC	total plant cost [€]
U_a	percentage of air utilisation [%]
U_f	percentage of fuel utilisation [%]
$\dot{W}_j$	brake power requirement/output of equipment j [kW_{el}]
WGS	water gas shift
WGSR	water gas shift reaction

Subscripts

0	reference value
ArC	air compressor
AGR	acid gas removal

Cite this work using DOI: 10.1016/j.ijggc.2021.103436

ASU	air separation unit
BRKP	brake power
calc	calciner
cap	pulp and paper plant with CO_2 capture
carb	carbonator
Claus	Claus sulphur plant
CCU	CO_2 compression unit
COND	condenser
DG	dry gas
eq	equivalent
ECON	economiser
FC	fuel compressor
FP	fuel preparation
H_2Comp	H_2 compressor at 60 bar
H_2PV	H_2 pressure vessel
H_2StorComp	H_2 compressor at 700 bar
HPW	high-pressure water
HRSG	heat recovery steam generator
LS	live steam
OXPH	oxygen preheater
ref	reference pulp and paper plant without CO_2 capture
SC	steam cycle
SGE	syngas expander
SST	small steam turbine

Cite this work using DOI: 10.1016/j.ijggc.2021.103436

REFERENCES

Akbari, M., Oyedun, A.O., Kumar, A., 2018. Ammonia production from black liquor gasification and co-gasification with pulp and waste sludges: A techno-economic assessment. Energy 151, 133–143. https://doi.org/10.1016/j.energy.2018.03.056

Andersson, J., Furusjö, E., Wetterlund, E., Lundgren, J., Landälv, I., 2016. Co-gasification of black liquor and pyrolysis oil: Evaluation of blend ratios and methanol production capacities. Energy Convers. Manag. 110, 240–248. https://doi.org/10.1016/j.enconman.2015.12.027

Andersson, J., Lundgren, J., Marklund, M., 2014. Methanol production via pressurized entrained flow biomass gasification - Techno-economic comparison of integrated vs. stand-alone production. Biomass and Bioenergy 64, 256–268. https://doi.org/10.1016/j.biombioe.2014.03.063

Armbrust, N., Duelli, G., Dieter, H., Scheffknecht, G., 2015. Calcium looping cycle for hydrogen production from biomass gasification syngas: Experimental investigation at a 20 kW_{th} dual fluidized-bed facility. Ind. Eng. Chem. Res. 54, 5624–5634. https://doi.org/10.1021/acs.iecr.5b00070

Atsonios, K., Koumanakos, A., Panopoulos, K.D., Doukelis, A., Kakaras, E., 2013. Techno-economic comparison of CO_2 capture technologies employed with natural gas derived GTCC, in: Proceedings of the ASME Turbo Expo. p. V002T07A018. https://doi.org/10.1115/GT2013-95117

Bank of England, 2019. Bank of England Statistical Interactive Database | Interest & Exchange Rates | Official Bank Rate History [WWW Document]. URL http://www.bankofengland.co.uk/boeapps/iadb/repo.asp (accessed 12.5.19).

BEIS, 2019. Industrial electricity prices in the EU. Business Energy & Industrial Strategy, United Kingdom.

Carlsson, P., Wiinikka, H., Marklund, M., Grönberg, C., Pettersson, E., Lidman, M., Gebart, R., 2010. Experimental investigation of an industrial scale black liquor gasifier. 1. The effect of reactor operation parameters on product gas composition. Fuel 89, 4025–4034. https://doi.org/10.1016/j.fuel.2010.05.003

Carvalho, L., Lundgren, J., Wetterlund, E., Wolf, J., Furusjö, E., 2018. Methanol production via black liquor co-gasification with expanded raw material base – Techno-economic assessment. Appl. Energy 225, 570–584. https://doi.org/10.1016/j.apenergy.2018.04.052

CEPCI, 2020. The Chemical Engineering Plant Cost Index [WWW Document]. Chem. Eng. URL https://www.chemengonline.com (accessed 12.5.19).

Connell, D.P., Lewandowski, D.A., Ramkumar, S., Phalak, N., Statnick, R.M., Fan, L.-S., 2013. Process simulation and economic analysis of the Calcium Looping Process (CLP) for hydrogen and electricity production from coal and natural gas. Fuel 105, 383–396. https://doi.org/10.1016/j.fuel.2012.07.006

Darmawan, A., Ajiwibowo, M.W., Yoshikawa, K., Aziz, M., Tokimatsu, K., 2018. Energy-efficient recovery of black liquor through gasification and syngas chemical looping. Appl. Energy 219, 290–298. https://doi.org/10.1016/j.apenergy.2018.03.033

De Lena, E., Spinelli, M., Gatti, M., Scaccabarozzi, R., Campanari, S., Consonni, S., Cinti, G., Romano, M.C., 2019. Techno-economic analysis of calcium looping processes for low CO_2

emission cement plants. Int. J. Greenh. Gas Control 82, 244–260. https://doi.org/10.1016/j.ijggc.2019.01.005

DOE/NETL, 2014. Baseline Analysis of Crude Methanol Production from Coal and Natural Gas, National Energy Technology Laboratory.

DOE/NETL, 2010. Assessment of hydrogen production with CO_2 capture volume 1: baseline state-of- the-art plants.

Doherty, W., Reynolds, A., Kennedy, D., 2010. Computer simulation of a biomass gasification-solid oxide fuel cell power system using Aspen Plus. Energy 35, 4545–4555. https://doi.org/10.1016/j.energy.2010.04.051

Eichman, J., Townsend, A., Melaina, M., 2016. Economic Assessment of Hydrogen Technologies Participating in California Electricity Markets. Golden, CO (United States), United States. https://doi.org/10.2172/1239543

Ekbom, T., Lindblom, M., Berglin, N., Ahlvik, P., 2003. Technical and commercial feasibility study of black liquor gasification with methanol/DME production as motor fuels for automotive uses – BLGMF, EU ALTENER program report. Stockholm, Sweden. https://doi.org/Contract No. 4.1013/Z/01-087/2001

Ferreira, E.T.D.F., Balestieri, J.A.P., 2015. Black liquor gasification combined cycle with CO_2 capture – Technical and economic analysis. Appl. Therm. Eng. 75, 371–383. https://doi.org/10.1016/j.applthermaleng.2014.09.026

Fuss, S., Canadell, J.G., Peters, G.P., Tavoni, M., Andrew, R.M., Ciais, P., Jackson, R.B., Jones, C.D., Kraxner, F., Nakicenovic, N., Le Quéré, C., Raupach, M.R., Sharifi, A., Smith, P., Yamagata, Y., 2014. Betting on negative emissions. Nat. Clim. Chang. 4, 850–853. https://doi.org/10.1038/nclimate2392

Gerres, T., Chaves Ávila, J.P., Llamas, P.L., San Román, T.G., 2019. A review of cross-sector decarbonisation potentials in the European energy intensive industry. J. Clean. Prod. 210, 585–601. https://doi.org/10.1016/j.jclepro.2018.11.036

Gil, M. V., Fermoso, J., Rubiera, F., Chen, D., 2015. H2 production by sorption enhanced steam reforming of biomass-derived bio-oil in a fluidized bed reactor: An assessment of the effect of operation variables using response surface methodology. Catal. Today 242, 19–34. https://doi.org/10.1016/j.cattod.2014.04.018

Hanak, D.P., Biliyok, C., Anthony, E.J., Manovic, V., 2015. Modelling and comparison of calcium looping and chemical solvent scrubbing retrofits for CO_2 capture from coal-fired power plant. Int. J. Greenh. Gas Control 42, 226–236. https://doi.org/10.1016/j.ijggc.2015.08.003

Hanak, D.P., Jenkins, B.G., Kruger, T., Manovic, V., 2017. High-efficiency negative-carbon emission power generation from integrated solid-oxide fuel cell and calciner. Appl. Energy 205, 1189–1201. https://doi.org/10.1016/j.apenergy.2017.08.090

International Energy Agency, 2020. The Future of Hydrogen, IEA. URL https://www.iea.org/reports/the-future-of-hydrogen (accessed 11.4.20).

Jafri, Y., Furusjö, E., Kirtania, K., Gebart, R., 2016. Performance of a Pilot-Scale Entrained-Flow Black Liquor Gasifier. Energy & Fuels 30, 3175–3185. https://doi.org/10.1021/acs.energyfuels.6b00349

Kreutz, T., Williams, R., Consonni, S., Chiesa, P., 2005. Co-production of hydrogen, electricity and CO from coal with commercially ready technology. Part B: Economic analysis. Int. J. Hydrogen Energy 30, 769–784. https://doi.org/10.1016/j.ijhydene.2004.08.001

Larson, E.D., Consonni, S., Katofsky, R.E., 2003. A Cost-Benefit Assessment of Biomass Gasification Power Generation in the Pulp and Paper Industry, October. Princeton University, Politecnico Milano, Navigant consulting.

Larson, E.D., Consonni, S., Katofsky, R.E., Iisa, K., Frederick, W.J., 2006. A Cost-Benefit Assessment of Gasification-Based Biorefining in the Kraft Pulp and Paper Industry.

Lee, Y.D., Ahn, K.Y., Morosuk, T., Tsatsaronis, G., 2014. Exergetic and exergoeconomic evaluation of a solid-oxide fuel-cell-based combined heat and power generation system. Energy Convers. Manag. 85, 154–164. https://doi.org/10.1016/j.enconman.2014.05.066

Lisbona, P., Martínez, A., Lara, Y., Romeo, L.M., 2010. Integration of Carbonate CO_2 Capture Cycle and Coal-Fired Power Plants. A Comparative Study for Different Sorbents. Energy & Fuels 24, 728–736. https://doi.org/10.1021/ef900740p

Manzolini, G., Macchi, E., Gazzani, M., 2013. CO_2 capture in natural gas combined cycle with SEWGS. Part B: Economic assessment. Int. J. Greenh. Gas Control 12, 502–509. https://doi.org/10.1016/j.ijggc.2012.06.021

Martínez, A., Lara, Y., Lisbona, P., Romeo, L.M., 2014. Operation of a mixing seal valve in calcium looping for CO_2 capture. Energy and Fuels 28, 2059–2068. https://doi.org/10.1021/ef402487e

Matuszny, K., Borhani, T.N., Nabavi, S.A., Hanak, D.P., 2020. Integration of solid-oxide fuel cells and absorption refrigeration for efficient combined cooling, heat and power production. Clean Energy 4, 328–348. https://doi.org/10.1093/ce/zkaa019

McGrail, B.P., Freeman, C.J., Brown, C.F., Sullivan, E.C., White, S.K., Reddy, S., Garber, R.D., Tobin, D., Gilmartin, J.J., Steffensen, E.J., 2012. Overcoming business model uncertainty in a carbon dioxide capture and sequestration project: Case study at the Boise White Paper Mill. Int. J. Greenh. Gas Control 9, 91–102. https://doi.org/10.1016/j.ijggc.2012.03.009

Michalski, S., Hanak, D.P., Manovic, V., 2019. Techno-economic feasibility assessment of calcium looping combustion using commercial technology appraisal tools. J. Clean. Prod. 219, 540–551. https://doi.org/10.1016/j.jclepro.2019.02.049

Millar, R.J., Fuglestvedt, J.S., Friedlingstein, P., Rogelj, J., Grubb, M.J., Matthews, H.D., Skeie, R.B., Forster, P.M., Frame, D.J., Allen, M.R., 2017. Emission budgets and pathways consistent with limiting warming to 1.5 °C. Nat. Geosci. 10, 741–747. https://doi.org/10.1038/NGEO3031

Mitsushima, S., Gollas, B., Hacker, V., 2018. Chapter 1 - Introduction, in: Hacker, V., Mitsushima, S. (Eds.), Fuel Cells and Hydrogen. Elsevier, pp. 1–13. https://doi.org/https://doi.org/10.1016/B978-0-12-811459-9.00001-3

Müller, C.R., Pacciani, R., Bohn, C.D., Scott, S.A., Dennis, J.S., 2009. Investigation of the enhanced water gas shift reaction using natural and synthetic sorbents for the capture of CO_2. Ind. Eng. Chem. Res. 48, 10284–10291. https://doi.org/10.1021/ie900772q

Naqvi, M., Yan, J., Dahlquist, E., 2013. System analysis of dry black liquor gasification based synthetic gas production comparing oxygen and air blown gasification systems. Appl. Energy 112, 1275–1282. https://doi.org/10.1016/j.apenergy.2012.11.065

Ni, M., 2006. An overview of hydrogen storage technologies. Energy Explor. Exploit. 24, 197–209. https://doi.org/10.1260/014459806779367455

Öhrman, O., Häggström, C., Wiinikka, H., Hedlund, J., Gebart, R., 2012. Analysis of trace components in synthesis gas generated by black liquor gasification. Fuel 102, 173–179. https://doi.org/10.1016/j.fuel.2012.05.052

Onarheim, K., Santos, S., Kangas, P., Hankalin, V., 2017. Performance and cost of CCS in the pulp and paper industry part 2: Economic feasibility of amine-based post-combustion CO_2 capture. Int. J. Greenh. Gas Control 66, 60–75. https://doi.org/10.1016/j.ijggc.2017.09.010

Perry, R., Green, D., Maloney, J., 2007. Perry's chemical engineers' handbook. New York: McGraw-Hill, USA.

Pettersson, K., Harvey, S., 2012. Comparison of black liquor gasification with other pulping biorefinery concepts – Systems analysis of economic performance and CO_2 emissions. Energy 37, 136–153. https://doi.org/10.1016/j.energy.2011.10.020

Pfeifer, C., Puchner, B., Hofbauer, H., 2007. In-Situ CO_2-Absorption in a Dual Fluidized Bed Biomass Steam Gasifier to Produce a Hydrogen Rich Syngas. Int. J. Chem. React. Eng. 5. https://doi.org/10.2202/1542-6580.1395

Ribeiro, A.M., Grande, C.A., Lopes, F.V.S., Loureiro, J.M., Rodrigues, A.E., 2008. A parametric study of layered bed PSA for hydrogen purification. Chem. Eng. Sci. 63, 5258–5273. https://doi.org/10.1016/j.ces.2008.07.017

Rogelj, J., Popp, A., Calvin, K. V., Luderer, G., Emmerling, J., Gernaat, D., Fujimori, S., Strefler, J., Hasegawa, T., Marangoni, G., Krey, V., Kriegler, E., Riahi, K., Van Vuuren, D.P., Doelman, J., Drouet, L., Edmonds, J., Fricko, O., Harmsen, M., Havlík, P., Humpenöder, F., Stehfest, E., Tavoni, M., 2018. Scenarios towards limiting global mean temperature increase below 1.5 °C. Nat. Clim. Chang. 8, 325–332. https://doi.org/10.1038/s41558-018-0091-3

Romano, M., Martínez, I., Murillo, R., Arstad, B., Bloom, R., Ozcan, D.C., H., A., Brandani, S., 2012. Process simulation of Ca-looping processes: Review and guidelines, 2013, in: 11th International Conference on Greenhouse Gas Control Technologies, GHGT 2012. Kyoto, Japan, pp. 18–22. https://doi.org/10.13140/RG.2.1.1453.5847

Sanna, A., 2014. Advanced Biofuels from Thermochemical Processing of Sustainable Biomass in Europe. Bioenergy Res. 7, 36–47. https://doi.org/10.1007/s12155-013-9378-4

Santos, M.P.S., Manovic, V., Hanak, D.P., 2021. Unlocking the potential of pulp and paper industry to achieve carbon-negative emissions via calcium looping retrofit. J. Clean. Prod. 280, 124431. https://doi.org/10.1016/j.jclepro.2020.124431

Shirazi, A., Aminyavari, M., Najafi, B., Rinaldi, F., Razaghi, M., 2012. Thermal–economic–environmental analysis and multi-objective optimization of an internal-reforming solid oxide fuel cell–gas turbine hybrid system. Int. J. Hydrogen Energy 37, 19111–19124. https://doi.org/10.1016/j.ijhydene.2012.09.143

Spallina, V., Motamedi, G., Gallucci, F., van Sint Annaland, M., 2019. Techno-economic assessment of an integrated high pressure chemical-looping process with packed-bed reactors in large scale hydrogen and methanol production. Int. J. Greenh. Gas Control 88, 71–84. https://doi.org/10.1016/j.ijggc.2019.05.026

Spallina, V., Pandolfo, D., Battistella, A., Romano, M.C., Van Sint Annaland, M., Gallucci, F., 2016. Techno-economic assessment of membrane assisted fluidized bed reactors for pure H2 production with CO_2 capture. Energy Convers. Manag. 120, 257–273. https://doi.org/10.1016/j.enconman.2016.04.073

Vogl, V., Åhman, M., Nilsson, L.J., 2018. Assessment of hydrogen direct reduction for fossil-free steelmaking. J. Clean. Prod. 203, 736–745. https://doi.org/10.1016/j.jclepro.2018.08.279

Whitty, K., 2005. Black Liquor Gasification: Development and Commercialization Update, in: ACERC Annual Conference. Provo Utah.

Wiranarongkorn, K., Arpornwichanop, A., 2017. Analysis of the Ca-looping sorption-enhanced steam reforming and solid oxide fuel cell integrated process using bio-oil. Energy Convers. Manag. 134, 156–166. https://doi.org/10.1016/j.enconman.2016.12.025

Yang, Y., Zhai, R., Duan, L., Kavosh, M., Patchigolla, K., Oakey, J., 2010. Integration and evaluation of a power plant with a CaO-based CO_2 capture system. Int. J. Greenh. Gas Control 4, 603–612. https://doi.org/10.1016/j.ijggc.2010.01.004

Zhang, G., Yan, J., Jin, H., Dahlquist, E., 2011. Integrated Black Liquor Gasification Polygeneration System with CO2 Capture in Pulp and Paper Mills to Produce Methanol and Electricity. Int. J. Green Energy 8, 275–293. https://doi.org/10.1080/15435075.2010.550077

Zhang, W., Croiset, E., Douglas, P.L., Fowler, M.W., Entchev, E., 2005. Simulation of a tubular solid oxide fuel cell stack using AspenPlus^{TM} unit operation models. Energy Convers. Manag. 46, 181–196. https://doi.org/10.1016/j.enconman.2004.03.002

Cite this work using DOI: 10.1016/j.ijggc.2021.103436

DR HANAK'S GROUP

Dr Hanak's group in Sustainable Energy and Process Engineering is an ambitious team of researchers working in the area combining power, process and environmental engineering with economics and computer science to solve global challenges and develop innovative solutions to meet sustainable development goals.

Specialities

- Process design and optimization
- Techno-economic assessment
- Environmental life-cycle assessment
- Carbon footprint assessment
- Uncertainty and risk assessment
- Machine learning for engineering assessment

Research areas

- Carbon capture and utilization
- Direct air capture
- Advanced power generation
- Industrial decarbonization
- Hydrogen production
- Assessment framework standarisation

Dr Dawid Hanak, MBA, CEng MIMechE, CMgr FCMI, FHEA
Senior Lecturer in Energy and Process Engineering, Cranfield University
For collaboration, contact me at contact@drhanak.com
Follow my groups updates on www.drhanak.com and LinkedIn

https://dspace.org/

Black liquor gasification with calcium looping for carbon-negative pulp and paper industry

Santos, Mónica P. S.; Manovic, Vasilije; Hanak, Dawid P.

2021-08-26
Elsevier
https://doi.org/10.1016/j.ijggc.2021.103436
Santos MP, Manovic V, Hanak DP. (2021) Black liquor gasification with calcium looping for carbon-negative pulp and paper industry. International Journal of Greenhouse Gas Control, Volume 110, September 2021, Article number 103436

Downloaded from a DSpace repository. https://dspace.org/